Layer Structures. 4. Role of Long Alkane Spacers in Poly(ester imide)s Derived from *N*-(4′-Hydroxyphenyl)-4-hydroxyphthalimide

Hans R. Kricheldorf,* Nicolas Probst, Gert Schwarz, and Christoph Wutz

Institut für Technische und Makromolekulare Chemie der Universität Hamburg, Bundesstrasse 45, D-20146 Hamburg, Germany

Received October 12, 1995; Revised Manuscript Received March 25, 1996[⊗]

ABSTRACT: Several polyesters were prepared from *N*-(4′-hydroxyphenyl)-4-hydroxyphthalimide and various alkanedicarboxylic acids. The dicarboxylic acids contained 12, 14, and 20 methylene groups. Optical microscopy, DSC, and X-ray measurements at variable temperatures revealed that the poly(ester imide)s (PETs) containing up to 10 CH_2 groups form a enantiotropic nematic phase, whereas those PEIs with 12 or more CH_2 groups form only a monotropic LC phase upon rapid cooling. All of these PEIs form a crystalline state with a smectic E-like layer structure, which undergoes a reversible change upon heating and cooling. Another interesting result is the predominance of transconformations of the spacers, as revealed by ^{13}C NMR CP/MAS spectroscopy. Copolymers were synthesized from 1:1 mixtures of $n = 20$ and $n = 12$ spacers or $n = 20$ and $n = 7$ spacers. They form an enantiotropic nematic phase, but again smectic layer structures in the solid state. The conformations of the spacers in both copolymers show different behavior. Whereas heating of the 20 + 12 copolymer favors gauche conformations and a rapid exchange with the trans conformation, the exchange between gauche and trans is extremely slow in the case of the 20 + 7 copolymer, because the $n = 20$ spacers are almost fully extended. Furthermore, the layer model of the 20 + 7 copolymer requires a dispersion of imide mesogens in the spacer layer.

Introduction

The present work is part of a broader study of polymers forming layer structures in general and poly(ester imide)s (PEIs) in particular. In a previous publication,[1] poly(ester imide)s of structure **1** have been described as made up by dicarboxylic acids with up to 11 CH_2 groups (**1a**−**i**). It was found that all of these poly(ester imide)s form an enantiotropic nematic phase in addition to a crystalline solid state with a smectoid layer structure. The formation of a nematic phase by the poly(ester imide)s **1a**−**i** is quite unusual, because regular sequences of polar imide groups and alkane spacers possess a high potential to form layer structures.[2−9] Particularly interesting are the largely different properties of the isomeric poly(ester imide)s **2a**−**h**. These poly(ester imide)s can adopt a smectoid crystalline phase, a smectic B phase, and a monotropic and a frozen smectic A phase, but never a nematic phase.[2,3] The present work reports on the synthesis and properties of poly(ester imide)s **1k**−**m** containing long spacers.

The purpose of this study was to determine whether the longer spacers favor the formation of a smectic LC phase at the expense of the nematic phase typical for the shorter spacers (**1a**−**i**). Furthermore, the properties of copolymers containing two spacers of different length should be studied. The influence of mixed spacers on the structure and stability of layer structures is an interesting probelm that has already been studied[6] and will be discussed further in future parts of this series. In this connection, a recent publication of Watanabe and co-workers on "frustrated layers" should be mentioned.[10] Conformational studies of aliphatic spacers in nematic polyesters have been reported by several authors.[11−13]

Experimental Section

Materials. 4-Hydroxyphthalic acid was a gift of Bayer AG (Leverkusen, Germany). Its anhydride, *N*-(4′-hydroxyphenyl)-4-hydroxyphthalimide (mp 300−302 °C), and its O,O′-bis-(trimethylsilyl) derivative (mp 86−88 °C) were prepared as described previously.[1] Dodecanedicarboxylic acid and tetradecanedicarboxylic acid were purchased from Aldrich Co. (Milwaukee, WI). Eicosa-10,12-diynedicarboxylic acid was purchased from Lancaster Synth. (D-63165 Mülheim/Main, Germany). It was hydrogenated in 1,4-dioxane at 25 °C in the presence of 5% Pt on charcoal. The isolated eicosane-α,ω-dicarboxyic acid was recrystallized from ethanol (mp 124 °C; mp 119−125 °C in ref 14).

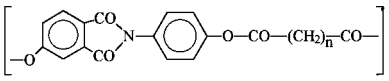

1a-m

a: n = 3 **e**: n = 7 **i**: n = 11
b: n = 4 **f**: n = 8 **k**: n = 12
c: n = 5 **g**: n = 9 **l**: n = 14
d: n = 6 **h**: n = 10 **m**: n = 20

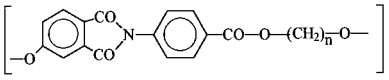

2a-h

a: n = 4 **d**: n = 7 **g**: n = 10
b: n = 5 **e**: n = 8 **h**: n = 12
c: n = 6 **f**: n = 9 **i**: n = 16
k: n = 22

Polycondensations. *N*-(4′-Acetoxyphenyl)-4-acetoxyphthalimide (20 mmol), an α,ω-dicarboxylic acid (20 mmol), and MgO (10 mg) were weighed into a cyclindrical glass reactor equipped with a stirrer and gas-inlet and gas-outlet tubes. This reactor was placed in an oil bath preheated to 150 °C. The temperature was raised in steps of 20 °C to the final reaction temperature over a period of approximately 8 h. The maximum temperature was maintained for 2 h in vacuo. The cold polymers were dissolved in a mixture of CH_2Cl_2 and trifluoroacetic acid (volume ratio 4/1) and precipitated into cold methanol. The isolated polymers were dried at 60 or 115 °C. In the latter case, an annealing effect with improvement in the crystallinity is observable.

Measurements. The inherent viscosities were measured with an automated Ubbelohde viscometer thermostated at 20 °C. The IR spectra were recorded with KBr pellets on a Nicolet SXB-20 FT-IR spectrometer. The 100 MHz ^1H NMR spectra were recorded with a Bruker AC-100 FT NMR spectrometer

[⊗] Abstract published in *Advance ACS Abstracts,* May 1, 1996.

S0024-9297(95)01525-7 CCC: $12.00

Table 1. Yields and Properties of Poly(ester imide)s Prepared from *N*-(4′-Acetoxyphenyl)-4-acetoxyphthalimide 4

polymer formula	yield (%)	η_{inh}[a] (dL/g)	elemental formula (formula weight)	elemental analyses	C	H	N
1k ($n = 12$)	93	0.28	$C_{28}H_{31}NO_6$	calcd	70.42	6.54	2.93
			(477.6)	found	69.65	6.63	3.03
1l ($n = 14$)	91	0.28	$C_{30}H_{35}NO_6$	calcd	71.26	6.98	2.77
			(505.6)	found	71.30	7.27	2.67
1m ($n = 20$)	96	0.30	$C_{36}H_{47}NO_6$	calcd	73.31	8.03	2.38
			(589.7)	found	72.99	8.18	2.47
3a ($n = 7 + 20$)	93	0.42	$C_{59}H_{68}N_2O_{12}$	calcd	71.06	6.87	2.81
			(997.1)	found	70.95	7.05	3.00
3b ($n = 12 + 20$)	94	0.41	$C_{64}H_{78}N_2O_{12}$	calcd	72.02	7.37	2.63
			(1067.3)	found	71.91	7.32	2.75

[a] Measured at 20 °C with $c = 2$ g/L in CH_2Cl_2/trifluoroacetic acid (volume ratio 9/1).

in 5 mm o.d. sample tubes. The DSC measurements were conducted with a Perkin-Elmer DSC-7 in aluminum pans under nitrogen. The WAXD powder patterns were recorded with a Siemens D-500 diffractometer using Ni-filtered Cu Kα radiation. The synchrotron radiation measurements were conducted with a wavelength of 1.5 Å at HASYLAB, DESY (Hamburg). A heating rate of 10 °C/min and a position-sensitive one-dimensional detector were used.

Results and Discussion

Syntheses. All poly(ester imide)s of this work were prepared by polycondensation of acetylated *N*-(4′-hydroxyphenyl)-4-hydroxyphthalic acid[1] with free dicarboxylic acids (eq 1). The dodecanedicarboxylic acid and

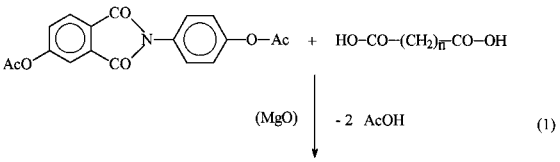

1k (n=12), 1l (n=14), 1m (n=20)

tetradecanedicarboxylic acid used for this purpose were commercial products. The eicosanedicarboxylic acid was prepared by Pt-catalyzed hydrogenation of the commercial eicosa-10-12,-diynedicarboxylic acid (eq 2). In

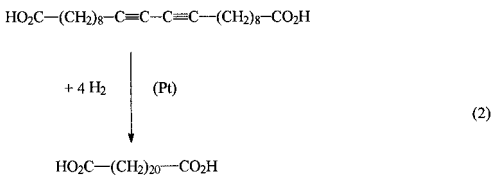

addition to the three homopoly(ester imide)s **1k**, **1l**, two copolymers (**3a** and **3b**) were synthesized. The yields, viscosities, and elemental properties of all PEIs are summarized in Table 1. Furthermore, IR spectra and ^{1}H NMR spectra were recorded, which agreed with the expected structures. Since neither IR nor NMR spectra of PEIs **1a**−**m** have ever been published before, the IR spectrum in Figure 1 should serve as a representative example.

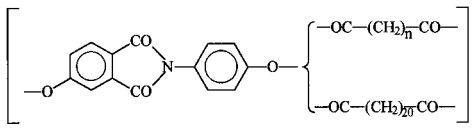

3a, b

a: n = 7 b: n = 12

Properties of the Homo-PEIs 1k−m. The WAXD powder patterns and DSC measurements agree that the homopoly(ester imide)s **1k**−**m** (like **1a**−**i**) are semicrystalline (see the following). The optical microscopy (with crossed polarizers) of **1k** correspondingly revealed a melting process at 180−185 °C, with the formation of an isotropic melt. In a very narrow temperature range of 4−5 °C, a liquid crystalline phase seemed to appear, but the presence of birefringent crystallites did not allow a clearcut identification. However, upon cooling a nematic melt with its typical threaded Schlieren texture appeared over a broader temperature range. Slow cooling from the isotropic melt yielded nematic droplets between 175 and 180 °C (Figure 2). These round droplets display the Schlieren texture and are less viscous than the surrounding isotropic phase. Poly(ether imide)s or poly(ester imide)s forming a smectic A phase may also form a kind of birefringent droplets upon slow cooling from the isotropic melt, yet those droplets are lengthy and yield a bâttonet texture upon short annealing. Furthermore, the smectic A phase is more viscous than the surrounding isotropic melt.

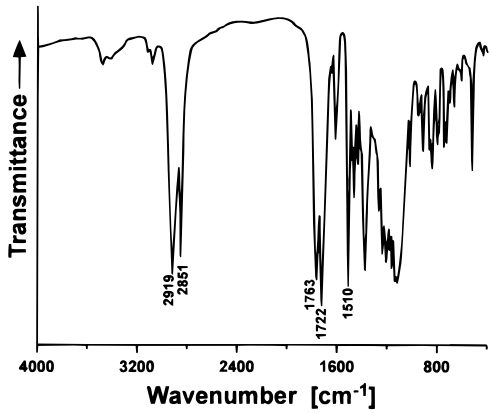

Figure 1. IR spectrum of PEI **1k**.

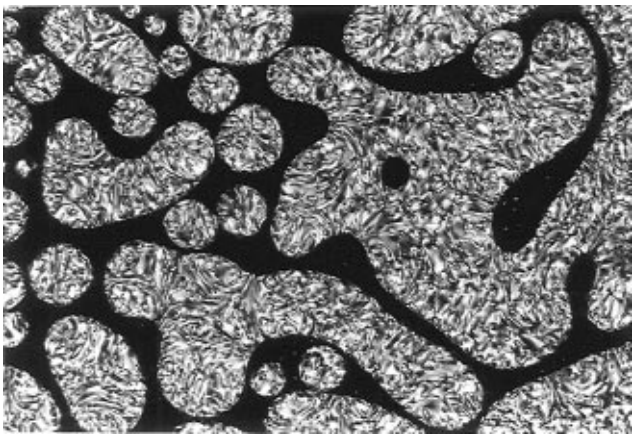

Figure 2. Nematic Schlieren texture of the homopoly(ester imide) **1k** formed between 175 and 180 °C upon cooling from the isotropic melt.

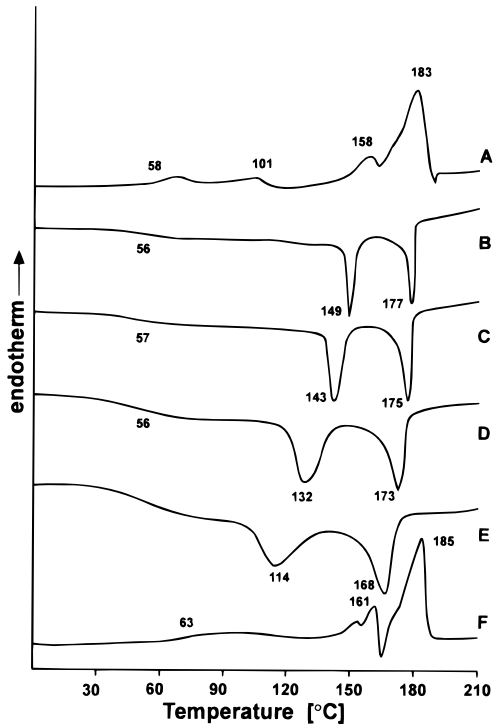

Figure 3. DSC measurements of PEI **1k**: (A) first heating with ±20 °C/min; (B) first cooling with −10 °C/min; (C) second cooling with −20 °C/min; (D) third cooling with −40 °C/min; (E) fourth cooling with −80 °C/min; (F) second heating after cooling with −20 °C/min.

Thus, **1k** clearly forms a nematic phase upon cooling, in perfect agreement with the observation of enantiotropic nematic phases in the case of **1a**−**i**. The temperature range of the monotropic nematic phase of **1k** depends on the cooling rate, as demonstrated by the DSC measurements of Figure 3.

In the case of **1l** and **1m**, neither an enantiotropic nor a monotroic LC phase was detectable by optical microscopy upon slow heating or cooling (up to 10 °C/min). However, DSC measurements with variation in the cooling rate demonstrated that a short-lived LC phase is formed upon rapid cooling (Figure 4). Thus, these observations fit well with the extrapolation of melting and isotropization temperatures of PEIs **1a**−**i** outlined in Figure 5. In other words, the increasing length of the spacer favors the crystalline state at the expense of the nematic phase, and it favors the rate of crystallization due to higher segmental mobility. This kinetic effect is evident from the weaker supercooling effect of the crystallization exotherm (e.g., in Figures 3 and 4). In this connection, a thermodynamic analysis of the stability of LC phases with regard to the molecular weight of LC main chain polymers should be mentioned.[15]

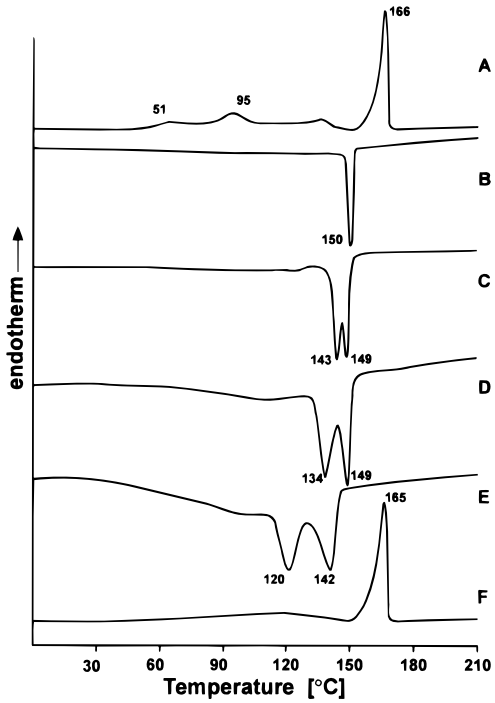

Figure 4. DSC measurements of PEI **1m**: (A) first heating with ±20 °C/min; (B) first cooling with −10 °C/min; (C) second cooling with −20 °C/min; (D) third cooling with −40 °C/min; (E) fourth cooling with −80 °C/min; (F) second heating after cooling with −20 °C/min.

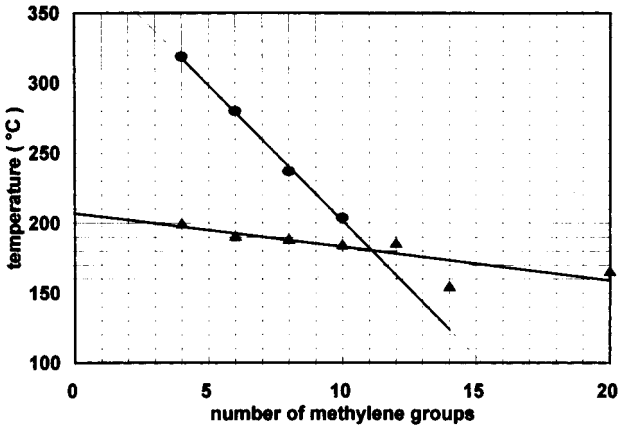

Figure 5. Plot of melting temperatures (T_m) and isotropization temperatures of PEIs **1** with even-numbered spacers.

The question that remains is which kind of solid state is formed by the PEIs **1a**−**m**. It has already been demonstrated for **1g** and **1h** in a previous paper that these PEIs adopt a smectic layer structure in the solid state. The WAXD powder patterns of **1k**−**m** confirm this interpretation (Figure 6A,B). A sharp middle angle reflection (MAR) is detectable, which allows the calcula-

Table 2. Thermal Properties of Poly(ester imide)s 1k−m, 3a, and 3b

polymer formula	*n*	T_g[a] (°C)	T_m[a] (°C)	T_i[b] (°C)	T_a[a] (°C)	T_a[c] (°C)	T_c[a] (°C)
1k	12	63	183	183−188	175	180	143
1l	14	75	155	155−160			
1m	20	51	166	165−170	149	155	143
3a	7 + 20	68	157	162−165[d]	158	164	103 (112)
3b	12 + 20	61	158	161−169[d]	155	164	102 (118)

[a] From DSC measured with a heating/cooling rate of 20 °C/min. [b] From optical microscopy with a heating rate of +10 °C/min. [c] Anisotropization as observed by optical microscopy at a cooling rate of −10 °C/min. [d] Enantiotropic nematic phase and isotropic phase are coexistent.

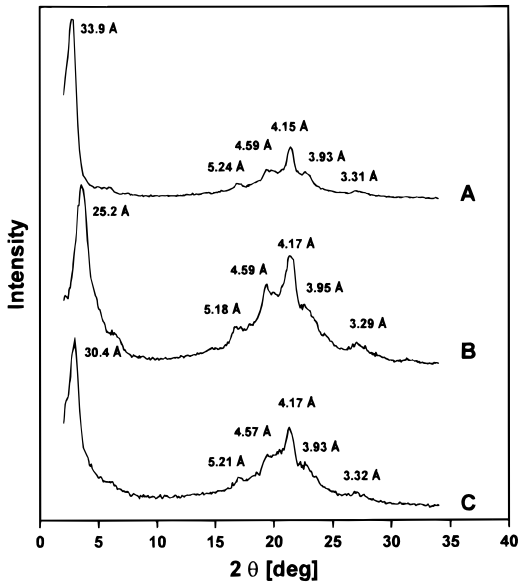

Figure 6. WAXD powder patterns of (A) PEI **1m**, (B) PEI **1k**, and (C) co-PEI **3b** measured after annealing at 115 °C.

Table 3. X-ray Reflections and Atomic Distances of PEI 1l (n = 14)

	WAXS		MAXS	
T (°C)	2θ	distance (Å)	2θ	distance (Å)
40	20.5	4.33	2.84	31.1
100	19.9	4.46	2.81	31.4
120	20.8	4.27	2.78	31.7
	18.9	4.69		
150	20.8	4.27	2.81	31.4
	18.7	4.74		

Table 4. X-ray Reflections and Atomic Distances of PEI 1m (n = 20)

	WAXS		MAXS	
T (°C)	2θ	distance (Å)	2θ	distance (Å)
40	20.6	4.31	2.58	34.20
			2.96	29.81
100	20.3	4.37	2.61	33.81
			2.96	29.81
140	19.6	4.52	2.61	33.81
			2.96	29.81
150	20.6	4.31	2.55	34.61
	18.9	4.69		
163	20.4	4.35	2.55	34.61
	18.6	4.76		

tion of the layer distance (d spacing) via the Bragg equation. A plot of the d spacings versus the number of CH_2 groups yields two interesting pieces of information (Figure 7). The first concerns the virtual length of the repeating unit with zero CH_2 groups. The value of 14 ± 0.5 Å is slightly longer than that of the mesogen (13.0 Å) calculated with one additional σ bond but without the CO groups. Therefore, this extrapolation clearly favors an upright position of the mesogens relative to the layer planes. With regard to the lateral order of the mesogens inside their layers, three scenarios may be considered: absence of any order, i.e., a frozen smectic A phase, hexagonal order, i.e., a smectic B phase, or orthorombic order, i.e., a smectic E type of layer structure. The wide angle reflection in the powder patterns of Figure 6A,B clearly indicates the existence of an orthorhombic (smectic E) type of order. Whether this smectic E type of layer structure is a mesophase or whether it may be called crystalline phase (with a long-range three-dimensional order) has not been studied in

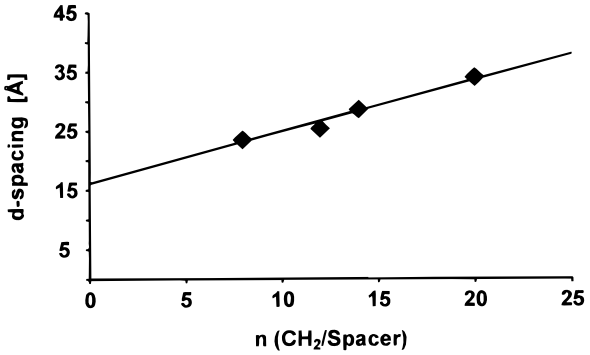

Figure 7. Plot of layer distances (d spacings) against the number of CH_2 groups in the spacers of PEIs **1a**−**m**.

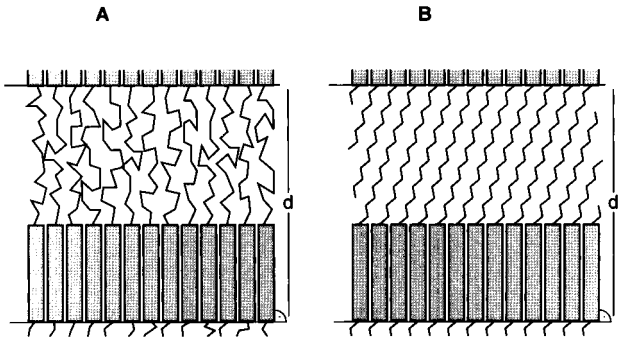

Figure 8. Layer models of PEIs **3k**−**m**: (A) upright spacers with an all-gauche conformation; (B) tilted spacers with an all-trans conformation.

this work. Regardless, the formation of a smectic E-like solid state is in good agreement with the properties of other poly(imide)s built up by regular sequences of imide mesogens and alkane spacers.[3,4,6,7,16]

The second piece of information concerns the conformation and chain packing of the spacers. The plot of d spacings versus CH_2 groups yields a slope of 0.95 ± 0.02 Å as the "pitch" of a CH_2 group. This value is much closer to that of an all-gauche conformation (0.90 Å) than to that of an all-trans conformation (1.27 Å). In other words, the X-ray data suggest at first glance that the gauche/trans ratio of the spacers is on the order of 8/2 or 9/1, provided that the spacers are in an upright position relative to the layer planes, as illustrated in Figure 8A. Fortunately, long aliphatic spacers have the advantage that ^{13}C NMR CP/MAS spectroscopy allows an experimental investigation of their conformations. In contrast to the layer model A (Figure 8), the ^{13}C NMR spectra clearly demonstrate that the trans conformation is predominant mainly in the case of **1k** and **1m** (Figure 9A). A chemical shift in the range of 33.0−33.5 ppm is characteristic for the all-trans conformation, whereas the shift range of 30.5−31.0 ppm represents trans−gauche combinations. Therefore, the layer model A needs revision and model B, with tilted spacers in an all-trans conformation, is obviously closer to the truth.

The ^{13}C NMR spectra of **1k**−**m** are also interesting from another point of view. Both ^{13}C CP/MAS and ^{2}H NMR spectra (of deuterated spacers) of the PEIs **2i,k**[17] and **4h,i**[9] agree in that part of their spacers form ordered paraffin domains between the layers of the mesogens. The chain segments inside the paraffin domains possess an all-trans conformation, and the exchange with the gauche conformations of spacers outside the paraffin domains is rather slow. The results obtained from **1k**−**m** indicate a completely different type of order and different chain dynamics in the spacer

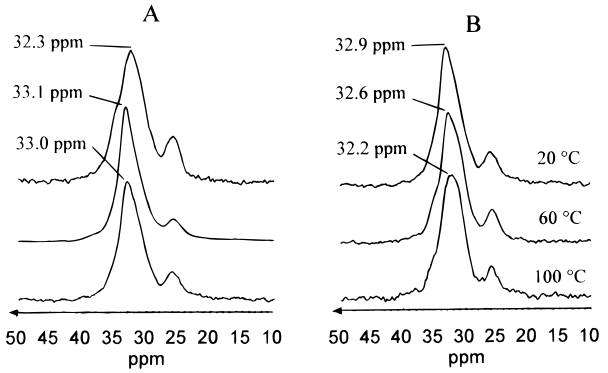

Figure 9. 75.4 MHz ^{13}C NMR spectra of PEIs: (A) PEIs **1k**, **1m**, and **3b** (from top to bottom); (B) co-PEI **3b** at different temperatures.

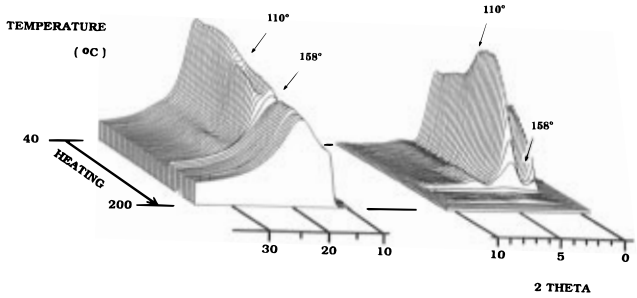

Figure 10. WAXS measurements of PEI **1k** conducted at a heating rate of 10 °C/min.

layers with a rapid exchange of gauche and trans conformations ($\nu_{ex} > 2.3\delta\nu = 350$ MHz). Upon heating, this exchange seems to accelerate and the fraction of gauche conformations increases. In other words, the conformational order and dynamics of long alkane spacers in smectic layers strongly depend on the nature of the mesogen, even when the chemical structure of the polymers is quite similar or isomeric.

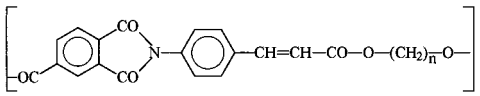

4a-i

a: n = 5 c: n = 7 e: n = 10 g: n = 12 i: n = 20
b: n = 6 d: n = 8 f: n = 12 h: n = 16

Finally, PEIs **1k**−**m** were subjected to synchrotron radiation measurements at a heating and cooling rate of 20 °C/min. For this purpose, samples were selected that were dried at 60 °C in a vacuum, in contrast to the samples used for the WAXS measurements of Figure 6. The WAXS powder patterns of these samples displayed, in addition to the MAR, only one broader nearly symmetrical reflection around $2\theta = 21°$. This pattern means that the PEIs exist in a kind of disordered smectic B or frozen smectic A phase. A sharp borderline between both scenarios does not exist. The "crystallization exotherm" in the cooling traces (Figures 3 and 4) indicates that the solid state formed upon rapid cooling or precipitation without annealing possesses a significant degree of order, which includes the formation of layers and possibly a conformational change in the spacers. Upon heating above 100 °C, the WA reflections of the "orthorhombic modification" (smectic E type) displayed in Figure 6 gradually appear and finally disappear upon melting (Figures 10 and 11). Figure 11 also illustrates that cooling from the isotropic melt at a rate of −20 °C/min does not allow a far-reaching

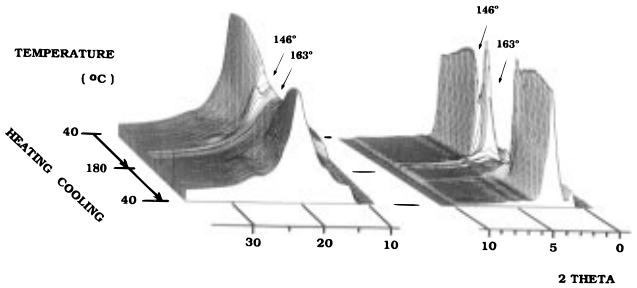

Figure 11. WAXS measurements of PEI **1m** conducted at a heating rate of 10 °C/min.

resaturation of the "orthorhombic modification". For the latter purpose, annealing above 100 °C is required. Finally, it is worth mentioning that the formation of the "orthorhombic modification" upon heating coincides with a sharpening of the MAR due to perfection of the layer structure. A more detailed analysis of chain packing and the influence of thermal history was not intended in the present work, but will be published separately.

Properties of Co-PEIs 3a and 3b. The co-PEIs **3a** and **3b** were synthesized to study the influence of a combination of two different spacers on the stability of the layer structures characteristic for the homo-PEIs. A similar study has been conducted with co-PEIs related to structure **2**. However, the properties of PEIs **2a**−**h** are so different from those of the series **1a**−**m** that no extrapolation from one series of PEIs to the other is allowed.

In the case of co-PEI **3a**, optical microscopy and DSC measurements agree that again an enantiotropic nematic phase exists between 154 and 169 °C. The temperature range of this phase is difficult to define for the heating process because of the broad melting process, which includes the coexistence of isotropic and nematic phases. However, two sharp exotherms appear in the cooling trace of the DSC measurements, indicating the appearance of the nematic phase (i.e., the anisotropization). Optical microscopy showed that the solidification coincides with a weak exotherm at 110 °C. In the case of **3b** a broad melting process with the formation of an enantiotropic nematic melt was also found by optical microscopy at temperatures in the range of 155−161 °C. Between 161 and 169 °C, an enantiotropic nematic phase was coexistent with the isotropic melt. Both optical microscopy and DSC measurements also confirmed the formation of a broad nematic phase upon cooling from the isotropic melt. Thus, these observations prove that the combination of short and long spacers destabilizes the smectic solid state and favors the formation of a nematic phase. In this connection, it should be mentioned that Roviello and Sirigu[18] have published a study of thermotropic (enantiotropic) copolyesters consisting of 4,4′-dihydroxy-α,α′-dimethylbenzalazine and two different α,ω-alkanedicarboxylic acids. In agreement with our results, a broadening of the temperature range of the nematic phase was found for a combination of spacers with six and ten CH_2 groups.

The co-PEIs **3a** and **3b** also have in common that rapid cooling (less than −20 °C/min) from the isotropic melt completely suppresses the crystallization of the mesogens. Interestingly, this failure of the mesogens does not prevent the formation of layer structures, as evidenced by the WAXS powder pattern of Figure 12A, even when the melt is quenched with ice. By assuming a more or less upright position of the mesogens, the solid

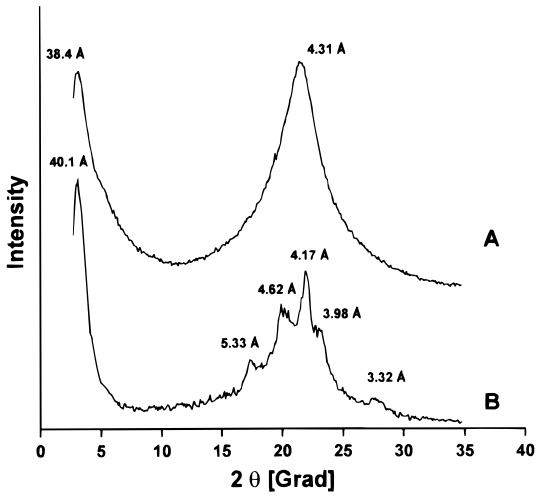

Figure 12. WAXS powder patterns of co-PEI **3a**: (A) after quenching from the isotropic melt; (B) after annealing for 24 h at 115 °C.

state of the quenched samples may be called a frozen smectic A phase. However, a clearcut distinction from a disordered smectic B phase again was not feasible. Analogous results were obtained by quenching of the PEIs **2a**−**h**.[3,6] This rapid formation of layer structures regardless of the order inside of the layers demonstrates the great tendency of poly(imide)s to form layer structures, provided that they consist of a regular sequence of imide groups and alkane spacers. Obviously, a regular pattern of polar and nonpolar building blocks is responsible for this phenomenon and allows its interpretation as a phase separation on the nanometer level.

When the quenched samples of **3a** or **3b** were annealed above T_g, highly ordered layer structures were formed as illustrated by Figure 12B. The mesogens adopt an orthorhombic array and the perfection of the layers increases, as demonstrated by the higher intensity and narrower line width of the MAR in analogy to the thermal properties of **1k**−**m**. The layer distance calculated from the MAR of **3b** amounts to 30.0−30.4 Å, a value that comes close to the length of the fully extended repeating unit (31 Å) calculated with an all-trans conformation of the $n = 12$ spacer. Considering a random sequence of both spacers, nearly 50 mol % of the shorter spacer should be present in every layer. Hence, the maximum layer distance is given by the fully extended shorter spacer. Correspondingly, the longer spacer is more or less coiled. The 100% gauche conformation of the $n = 20$ spacer in the scheme of Figure 13B is certainly an exaggeration with the purpose of illustrating the difference between both spacers. The ^{13}C NMR CP/MAS spectra revealed a higher than expected fraction of the trans conformation (Figure 9B), which shifts to a higher gauche content at higher temperatures (in analogy to the PEIs **1k**−**m**). According to this result, a sizable fraction of the CH_2CH_2 units of the $n = 20$ spacer adopt the trans conformation at room temperature, but the spectra do not give any indication of ordered paraffin domains. An analogous layer structure was found for a co-PEI of structure **2** containing a combination of $n = 8$ and $n = 12$ spacers.[6]

When a layer structure according to the model of Figure 13B is assumed for co-PEI **3a**, a maximum *d* spacing of 25 Å should be formed. However, the corresponding MAR does not appear in the X-ray pattern (Figure 12B). The sharp MAR found after

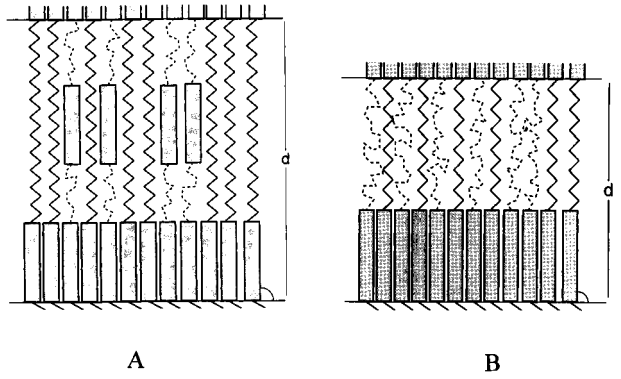

Figure 13. (A) Model for the layer structure of co-PEI **3a**. (B) Model of the layer structure of co-PEI **3b**.

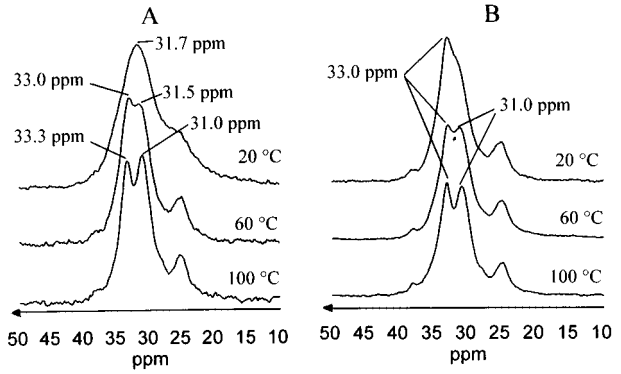

Figure 14. 75.4 MHz ^{13}C NMR CP/MAS spectra of co-PEI **3a**: (A) sample quenched from the isotropic melt; (B) sample annealed at 115 °C.

annealing represents a *d* spacing of 40 Å, which comes close to the length of a fully extended repeating unit of **1m** (41 Å) with the spacer in the all-trans conformation. This result is surprising at first glance because such a layer cannot integrate the short ($n = 7$) spacer in the usual way. A hypothetical explanation is given by the layer model of Figure 13A. Most of the long spacers are almost fully extended, whereas the short spacers and part of the long spacers are more or less coiled or folded. The most conspicuous aspect of this layer model is the assumption of imide mesogens being dispersed in the "soft layer". From this point of view, this layer model resembles classical domain structures, which are well-known to contain individual hard segments dispersed in the soft domains. The length of the mesogens of 13 Å (measured from O to O) is no hindrance for their accommodation in the "soft layer". Since the imide groups are highly polar, their molecular dispersion in the alkane phase is, of course, energetically highly unfavorable. Therefore, this model requires that several imide mesogens together form clusters. If these clusters are small and disordered, they will not contribute to the WAXS reflections. The WAXS reflections observable in Figure 12B agree with those of **1m** (Figure 6A) and, thus, exclusively originate from the well-ordered main layers of the mesogens.

The ^{13}C NMR CP/MAS spectra of co-PEI **3a** (Figure 14) demonstrate that the conformational situation of its layer structure is quite different from that of **3b**. The annealed sample displays the expected predominance of the trans conformation (Figure 14B). With increasing temperature, two populations of conformations and spacers become detectable. Obviously one sort of spacer adopts a stable all-trans conformation. Another group of spacers is more mobile, and their gauche/trans ratio increases at higher temperatures. The quenched sample

does not show a high content of trans conformations, and most spacers undergo a rapid exchange of gauche and trans conformations when measured at 20 °C (Figure 14A). However, two populations of spacers and conformations again become detectable at higher temperatures, obviously due to the annealing effect.

The layer model of Figure 13A allows a consistent interpretation of these spectroscopic results, which in turn support the layer model. The shorter layer distances and disorder of the layers in the quenched sample allow the long spacers to relax a little and to adopt gauche and trans conformations with rapid exchange. The annealing enhances the layer distances and stretches the long spacers. High temperatures intensify the motions of the mobile (coiled) fraction of spacers and mesogens dispersed in the "soft layer", which in turn press the layers of crystalline mesogens away from each other, thereby imposing more stress on the extended long spacers. If this interpretation is correct, it is a little suprising that spacers with a stable all-trans conformation are not detectable in the ^{13}C NMR CP/MAS spectrum of **3b** at 100 °C (Figure 9B). Possibly, the extended $n = 12$ spacers of **3b** are not clearly observable because the number of CH_2 groups of the coiled $n = 20$ spacers with conformation-sensitive chemical shift is greater by a factor of 2.3 (12−6 versus 20−6 CH_2 groups). A more detailed study of **3b** containing selectively deuterated spacers is in progress and will be published in the future.

Conclusion

The results of this work demonstrate that long alkane spacers connected to *N*-(4′-hydroxyphenyl)-4-hydroxyphthalimide favor the formation of crystalline layer structures at the expense of the nematic phase in the thermodynamic and in the kinetic sense. The layer structures of all PEIs correspond (after annealing) to a smectic E order. The combination of a long and a short spacer in a random sequence entails new types of layer structures, with a bimodal distribution of conformations. One sort of spacer is almost fully extended and adopts an all-trans conformation, whereas the other sort of spacer is more or less coiled. These results, combined with those of previous studies,[6,7,12] demonstrate that the layers of the alkane spacers in LC main chain polymers are far more complex than expected from low molar mass smectic compounds.

References and Notes

(1) de Abajo, J.; de la Campa, J.; Kricheldorf, H. R.; Schwarz, G. *Makromol. Chem*. **1990**, *191*, 537.
(2) Kricheldorf, H. R. *Mol. Cryst. Liq. Cryst*. **1994**, *87*, 254.
(3) Kricheldorf, H. R.; Schwarz, G.; de Abajo, J.; de la Campa, J. *Polymer* **1991**, *32*, 942.
(4) Pardey, R.; Wa, S. S.; Chen, J.; Harris, F.; Cheng, S. Z. D.; Aducci, J.; Facinelli, J. V.; Lenz, R. W. *Macromolecules* **1993**, *26*, 3687.
(5) de Abajo, J.; de la Campa, J.; Kricheldorf, H. R.; Schwarz, G. *Polymer* **1994**, *35*, 5577.
(6) Kricheldorf, H. R.; Schwarz, G.; Berghahn, M.; de Abajo, J.; de la Campa, J. *Macromolecules* **1994**, *27*, 2540.
(7) Kricheldorf, H. R.; Linzer, V. *Polymer* **1995**, *36*, 1893.
(8) Kricheldorf, H. R.; Berghahn, M. *J. Polym. Sci., Part A, Polym. Chem*. **1995**, *33*, 427.
(9) Kricheldorf, H. R.; Probst, N.; Wutz, Ch. *Macromolecules* **1995**, *28*, 7990.
(10) Watanabe, J.; Nakata, Y.; Simizu, K. *J. Phys. II, France* **1994**, *4*, 581.
(11) Mueller, K.; Hisyen, B.; Ringsdorf, H.; Lenz, R. W.; Kothe, G. *Mol. Cryst. Liq. Cryst*. **1984**, *113*, 167.
(12) Mueller, K.; Kothe, G. *Ber. Bunsenges. Phys. Chem*. **1985**, *89*, 1214.
(13) Leisen, J.; Boeffel, J.; Spiess, H. W.; Yoon, D. Y.; Sherwood, M. H.; Kawasumi, M.; Percec, V. *Macromolecules* **1995**, *28*, 6937.
(14) Signer, R.; Sprecher, P. *Helv. Chim. Acta* **1991**, *30*, 1003.
(15) Percec, V.; Keller, A. *Macromolecules* **1990**, *23*, 4347.
(16) Kricheldorf, H. R.; Gurau, M. *J. Polym. Sci., Part A, Polym. Chem*. **1995**, *33*, 2241.
(17) Kricheldorf, H. R.; Probst, N.; Domschke, A.; Wutz, Ch. *ACS Symp. Ser. 598*, Chapter 18.
(18) Roviello, A.; Sirigu, A. *Eur. Polym. J*. **1979**, *15*, 61.

MA951525S